Modelling groundwater evapotranspiration in a shallow aquifer in a semi-arid environment

Ousmane Coly Diouf[1*], Lutz Weihermüller[2], Mathias Diedhiou[1], Harry Vereecken[2], Seynabou Cissé Faye[1], Sérigne Faye[1], and Samba Ndao Sylla[3]

[1] Geology Department, Faculty of Sciences and Techniques, University Cheikh Anta Diop, Dakar, B.P 5005, Dakar-Fann, Senegal

[2] Forschungszentrum Jülich GmbH, Agrosphere Institute IBG-3, 52425 Jülich, Germany

[3] Department of Plant Biology, Faculty of Sciences and Techniques, University Cheikh Anta Diop, Dakar, B.P 5005, Dakar-Fann, Senegal

* Corresponding author: Geology Department, Faculty of Sciences and Techniques, University Cheikh Anta Diop, Dakar, B.P 5005, Dakar-Fann, Senegal;
email: ouscolydiouf@yahoo.fr; ousmanecoly.diouf@ucad.edu.sn

Abstract

The use of diurnal or seasonal water table fluctuation (WTF) to estimate groundwater evapotranspiration (ET_G) at different land uses and climate conditions is increasing applied in ecohydrological studies. In this study, we applied the WTF method for a shallow aquifer in an urbanized area in Senegal over the dry season 2000-2013.To analyze the applicability and validity of the WTF method for this site, and to understand the impact of the parameters used in this method, the unsaturated /saturated system was first simulated using the HYDRUS 1D model. The drawdown of the water table ranges from 18.1 to 113.2 cm and 10.4 to 101.9 cm for a bare soil and a perennial grass scenario and is highly related to the annual rainfall of the previous rainy season. The results indicate that the mean daily FAO-PM reference evapotranspiration rates for this area ranged from 2 to 4 mmd^{-1} and that the estimated actual evapotranspiration (ET_a) from the HYDRUS 1D model ranged between 0.22 to 1.11and 0.23 to 1.27 mmd^{-1} in bare soil and vegetative condition, respectively. ET_a and ET_G were well correlated for the vegetated scenario. However, the WTF method slightly overestimates ET_a fluxes in the bare soil scenario. The study shows that the decline of ET_a with water table depth can be simulated by an exponential function. The overall results indicate that higher ET_a values were observed when the water table is shallow, suggesting that ET_a is mainly driven by the water table depth at this site.

Keywords: evapotranspiration, water table fluctuation, semi-arid regions, unsaturated zone

1. Introduction

Sustainable management of groundwater resources requires detailed information of all components of the water budget such as precipitation, storage changes, recharge, as well as actual evapotranspiration (ET_a). Different approaches derived from climatic data are available to estimate potential reference evapotranspiration (ET_0) such as the physically based Penman-Monteith (PM) equation (Allen et al., 1998), simplified PM equation, and (semi-) empirical approach introduced by Thornthwaite (1948), Makkink (1957), Priestly-Taylor (1972), and Hargreaves and Samani (1985). Unfortunately, ET_a can only be calculated based on ET_0 using physically based models (Kollet et al., 2009). On the other hand, ET_a can be measured directly using the eddy correlation (EC) method, whereby the EC data have to be often corrected (e.g., Twine et al., 2000, Wilson et al., 2002) and gap filled (e.g., Moffat et al., 2007) resulting in errors in the ET_a estimation. Additionally, the EC method requires complex measurement systems, which are often not available at sites under investigation. Weighable lysimeters as another direct technique for estimating ET_a are also feasible (Meissner et al., 2007; Schrader et al., 2013; von Unold and Frank, 2008) but they need complex installation and maintenance.

It is known, that the shallow water table is directly influenced by ET_a through upward flow (e.g., Maxwell and Kollet, 2008; Vanderborght et al., 2010) and its temporal fluctuations in many arid/semi-arid regions express the response to evaporation and plant transpiration in the unsaturated zone (Loheide et al., 2005; Ridolfi et al., 2007). In these arid and semi-arid regions, groundwater evapotranspiration (ET_G) can be a predominant mechanism of seasonal groundwater fluctuations (Nichols, 1994; Healy and Cook, 2002). Accurate estimates of ET_G is difficult to obtain because of variability in local atmospheric conditions (Mazur et al., 2014), changing groundwater levels (Ridolfi et al., 2006), and spatially heterogeneous land use effects (Sanderson et al., 2008). Especially, the latter might have an important impact on ET_G estimates if the vegetation cover over the aquifer varies causing different transpiration

77 amounts. However, this estimation is needed to understand the implications of climate change
78 for water resource management and to develop adaptation strategies (Mazur et al., 2014).
79 The water table fluctuation (WTF) method, based on the premise that changes in the water
80 table of unconfined aquifers are caused by evapotranspiration only (Healy and Cook, 2002;
81 Lautz, 2008), has been widely used to estimate ET_G rates in arid and semi-arid areas (e.g.,
82 Carlson Mazur et al., 2014; Gribovszki et al., 2008; Soylu et al., 2012; Wang et al., 2014).
83 The advantage using this method is that water loss due to evapotranspiration is directly
84 measured through groundwater level changes and no additional instrumentation at the soil
85 surface is therefore needed (White, 1932; Meyboom, 1965; Gerla, 1992; Loheide et al., 2005).
86 The originally proposed WTF method as introduced by White (1932) was modified by several
87 authors due to uncertainties and deficiencies from different sources (e.g., Meyboom, 1965;
88 Engel et al., 2005; Gribovszki et al., 2008; Loheide, 2008), whereby the introduction of a term
89 accounting for the specific yield improved the performance of the White method substantially.
90 The specific yield, which is defined as the average amount of water per unit volume of soil
91 drained from a soil column extending from the water table to the ground surface per unit
92 lowering of the water table (Sophocleous, 1985), is highly variable in shallow water table
93 aquifers and it depends on soil texture, water table depth, and rate of change (Duke, 1972;
94 Sophocleous,1985; Healy and Cook,2002; Loheide, 2008; Gribovszki et al., 2010). In general,
95 a water level located below the rooting zone is a limitation for the application of the WTF
96 method (Mould et al., 2010). Other factor influencing the accuracy of ET_G estimation by the
97 WTF methods involves the inherent assumption that groundwater recovery rates are constant
98 over time despite that changes might occur over the course of the day, which are related to
99 changing evapotranspirative demand (Troxell, 1936). Because large part of the ET_a occurs
100 through transpiration (root water uptake), ET_G depends on the actual vegetation cover and its
101 status (Bethenod et al., 2000; Hsiao and Xu, 2005; Wilson et al., 2000). Finally, application of
102 the WTF method during rainy season is problematic because of the rapid rise in water table

103 elevation and subsequent percolation losses. To avoid storage changes within the unsaturated
104 zone due to precipitation many authors have chosen the dry periods to estimate ET_G (Wilson
105 et al., 2000; Mould et al., 2010).
106 As mentioned above, ET_G under none influenced system is mainly related to soil evaporation
107 and the direct water withdrawal by plants. However, in urbanized and agricultural zones daily
108 and seasonal groundwater fluctuations may be impacted by human activities such as
109 groundwater extraction for drinking or irrigation water. This water extraction from the
110 Quaternary sandy aquifer located in the region of Dakar had played a major role in supplying
111 drinking and irrigation water in the past, whereby the use of the groundwater started in the
112 1950s with periods of higher and lower exploitation ranging from 15.000 to 1.300 m^3 per day.
113 Within the last years, pumping was abandoned due to nitrate pollution resulting from
114 improper sanitation system in the urbanized area. On the other hand, the municipal authorities
115 currently discuss to allow pumping again to satisfy the water supply of gardening in the peri-
116 urban area.
117 Therefore, the objective of this study is to estimate the daily evapotranspiration rates to get
118 knowledge about potential groundwater recharge and potential sustainable future extraction
119 capacities. To do so, the ET_G rates form the WTF method were calculated and compared with
120 actual evapotranspiration data (ET_a) calculated by the physically based HYDRUS 1D model
121 for different surface covers, namely bare soil and savanna type grass vegetative in Western
122 Senegal.

123 **2. Materials and Methods**

124 **2.1. Study area**

125 The Dakar region extends over 550 km^2 between longitudes 16°55’ and 17°30’ west and
126 latitudes 14°55’ and 14°35’ north (Fig. 1). The region is characterized by a semi-arid climate
127 with a rainy season occurring from June to October. Annual rainfall varies strongly between
128 the years being for example 150 mm in 1983 and 723 mm in 2009, while the long-term mean

is 410 mm (1961-1990). Maximum air temperature is on average 29.5°C (1980-2010) and occurs from May to June and October to November corresponding to the beginning and the end of the rainy season. Minimum air temperature is observed during the period from December to February (18.5 °C). Daily mean FAO-PM reference evapotranspiration estimated between 2000 and 2013 ranged between 2 and 4 mm d^{-1}.

Geologically, the Dakar region belongs to the Senegalese-Mauritanian basin, the largest coastal basin of northwest Africa (Castalain, 1965), which is covered by Quaternary sediments of sandy and sandy clay nature from alluvial and eolien deposits (Bellion, 1987). This Quaternary sandy formation constitutes the groundwater reservoir in the Dakar region and it overlay the impermeable marly sediments of the Eocene. The top formations are made up by unleached tropical ferruginous soils locally called 'soil Diors' that represent 80%of the total area (Maignien, 1959). Additionally, hydromorphic and holomorphic soils are often located around the coastal lagoons. These soils are characterized by a significant presence of organic matter in the surface layer.

2.2. Soil sampling, field data, and laboratory measurements

Soil sampling was performed in the Dakar area in May 2015, whereby undisturbed soil cores using Kopecky rings of 250 cm^3 (height = 5 cm, diameter = 8.4 cm) were taken in the uppermost three soil horizons from the sampling depth of 0 - 25 (with n = 3), 25 - 100 (n = 3), and 100-200 cm (n = 4) and transferred to the Forschungszentrum Jülich GmbH, Germany for analysis. For the estimation of the hydraulic properties (Mualem van Genuchten parameters (van Genuchten, 1980)) the HYPROP® (METER Group, München, Germany) method as described by Schindler et al. (2010) was used in combination with the WP4®Dewpoint Potentiometer (Decagon Devices, WA, USA). The saturated hydraulic conductivity was estimated independently at the same samples using the falling head method by the Ksat device (METER Group, München, Germany).

Previously, unsaturated zone characterization was investigated in this study area using a hand auger device up to a depth of 300 cm. Soil samples were collected at 0.25 cm interval down to 1 m depth and beyond in 50 cm intervals down to the water table, which was at 250 cm depth. Samples were bulked and homogenized for each depth and gravimetric soil water contents were determined by drying 20 g of the sample at 110°C for 4 h. Additionally, particle size distributions were performed via sieve analysis (>50 µm fraction).

Groundwater level data in piezometer P3.1 located close to the investigated site (Fig. 1) were recorded using Thalimede Orpheus mini recorders (OTT Hydromet GmbH, Germany) during time period 2010 to 2012 in order to determine groundwater fluctuations over two dry seasons. The vegetation surrounding the groundwater well was grass vegetation but also bare patches were detectable, whereby the vegetation also depends on dry or wet season.

2.3.WTF method

The WTF method is usually applied in arid and semi-arid environments to estimate actual evapotranspiration fluxes by analyzing groundwater level changes in unconfined aquifers (White, 1932; Healy and Cook, 2002). The ET_G derived from this method can be expressed as (Wang et al., 2014):

$$ET_G = S_y \frac{\Delta H - \Delta h}{\Delta t} \quad [1]$$

where S_y is the specific yield [-], ΔH is the change of the groundwater level over the corresponding period [cm], Δh is the lateral flow [cm d^{-1}], and Δt is the time interval [day].

The overall change of the water table head [ΔH] is assumed to equal the overall water table change at the well between the beginning and the end of the dry season. In general, lateral flow [Δh] can be estimated by using the slope of the groundwater table curve before and after the growing season. In our region, lateral flow Δh can be neglected because the aquifer is located in a plain and because lateral flow is less important at the seasonal scale as pointed out by Pozdniakov et al. (2013). Therefore, equation [1] can be simplified to:

$$ET_G = S_y \frac{\Delta Z_y}{\Delta t} \quad [2]$$

where ΔZ_y is the seasonal decline of the groundwater table.

Crosbie et al. (2005) introduced the apparent specific yield (S_{ya}) term to evaluate the dynamics of the specific yield. The apparent specific yield can be calculated by the knowledge of the van Genuchten parameters (van Genuchten, 1980) by:

$$S_{ya} = S_{yu} - \frac{S_{yu}}{[1+(\propto(\frac{z_i+z_f}{2})^n]^{1-\frac{1}{n}}} \qquad S_{yu} = \theta_s - \theta_r \quad [3]$$

where θ_s and θ_r are the saturated and residual water contents [cm^3cm^{-3}], z_i and z_f are the initial and final depth to the water table [cm], and α [cm^{-1}] and n [-] are the van Genuchten parameters.

Equation [4] is used to calculate the average apparent specific yield S_{ya} when the groundwater table fluctuates in m soil layers.

$$\overline{S_{ya}} = \frac{\sum_{i=1}^{m} \Delta h_i S_{yi}}{\sum_{i=1}^{m} \Delta h_i} \qquad i = 1, 2, \ldots\ldots, m \quad [4]$$

where S_{yi} is the specific yield of the corresponding soil layer [-], and Δh_i is the amplitude of the groundwater level fluctuation in the i^{th} layer [cm].

2.4. Numerical Modeling

For the simulation of vertical water flow, the one-dimensional Richards equation (Eq.5) was solved using the finite element code HYDRUS 1D (Šimůnek et al., 2008; Šimůnek and van Genuchten, 2008):

$$\frac{\partial \theta_{(h)}}{\partial t} = \frac{\partial}{\partial z}\left[K_{(h)}\left(\frac{\partial h}{\partial z}+1\right)\right] - S \quad [5]$$

where θ is the volumetric water content [cm^3 cm^{-3}], h is the pressure head [cm], z represents the vertical coordinate [cm] positive in the downward direction, and $K_{(h)}$ is the unsaturated hydraulic conductivity as a function of pressure head [cm d^{-1}]. The sink term S in Eq. [5]

describes the volume of water removed from a unit volume of soil due to plant water uptake and is defined by Feddes et al. (1978) as:

$$S_{(h)} = \alpha_{(h)} S_P \quad [6]$$

where $\alpha_{(h)}$ is the root water uptake function and S_p is the potential water uptake rate (Šimůnek et al., 2008). The Mualem–van Genuchten functions (van Genuchten, 1980) were used to describe the relationship between θ, K and h with:

$$\theta_{(h)} = \theta_r + \frac{\theta_s - \theta_r}{\left(1 + |\alpha h|^n\right)^m} \quad [7]$$

$$K_{(h)} = K_s S_e^{0.5} \left[1 - \left(1 - S_e^{1/m}\right)^m\right]^2 \quad [8]$$

$$S_e = \frac{\theta - \theta_r}{\theta_s - \theta_r} \quad [9]$$

where S_e is the effective saturation [cm^3 cm^{-3}], θ_r and θ_s [cm^3 cm^{-3}] are the residual and saturated volumetric water contents, respectively, α [cm^{-1}], n [-], and m [-] (m = 1-1/n) are shape parameters, and K_s [cm d^{-1}] is the saturated hydraulic conductivity.

For the inverse modeling of the HYPROP® data, the model was setup in the same dimensions as the laboratory column and the flux over the upper surface (= normalized weight loss) was imposed at top boundary condition. Initialization was in pressure head with hydrostatic equilibrium from the lowest node (h_{bottom} = 0 cm). For the inversion the implemented Levenberg-Marquardt algorithm was used for the estimation of all hydraulic parameters of Eq. [7] and [8].

ET_a was simulated using HYDRUS 1D with the estimated HYPROP® hydraulic parameters for the Dakar region, whereby the simulation domain was assumed to be 2300 cm deep, assuming that the largest fraction of the domain was fully water filled (lowest ~ 2000 cm) and

acts as a groundwater reservoir, which will fluctuate over depth as a system response to infiltration and evapotranspiration. At the upper boundary, atmospheric inputs for daily precipitation and potential evapotranspiration were used from the years 2000-2013. The soil hydraulic parameters for each layer were taken from the inversion of the HYPROP® data. The groundwater hydraulic parameters were assumed to be a continuation of layer 3 because we considered that ET_a is more influenced by the upper than the deepest layers. The ratio of potential evaporation to transpiration was calculated based on the approach introduced by Simunek et al. (2008), where the potential transpiration (T_{pot}) and the potential evaporation (E_{pot}) can be separated by the knowledge of the leaf area index (LAI):

$$T_{pot} = ET_0(1 - e^{-k \times LAI}) \quad [10]$$

$$E_{pot} = ET_0\ (e^{-k \times LAI}) \quad [11]$$

where ET_0 is the reference evapotranspiration [cm], k is a parameter [-] that governs the radiation extinction of the canopy, which depends on the sun angle, the distribution of plants, and the arrangement of leaves. Here, we used k = 0.49 as a representative value for grassland (Simunek et al., 2008) and LAI was taken from Bobée et al. (2012) over the growing season.

An overview of the atmospheric forcing's (precipitation, potential evapotranspiration) and LAI is shown in Fig. 3 and 4. LAI varies between 0.27 to 0.8 m^2m^{-2} in natural herbaceous savanna type vegetation (closed to open >40%). Rainfall records were characterized by high frequency and intensity events producing high flooded area in the years 2005, 2008, 2009, 2010, and 2013. For example, in August 1st to 2nd, 13st to 19st, 22nd to 25th, and 28th to 30stof 2005, rainfall recorded equal 63.9, 108.9, 97.3, and 49.21 mm, respectively. This situation causes flooding of many districts in the peri-urban area, where groundwater level is highly related to rainfall events (Diouf et al., 2013). Maximum daily ET_0 calculated by FAO-PM was observed during the dry season, when the study area is influenced by the NE-SW hot and dry

247 wind locally called ‘harmattan’. Minimum values occur during the rainy season characterized
248 by high air humidity > 70%.
249 Root depth was set to be 100 cm according to February and Higgins (2010) and due to the
250 perennial grassland vegetation no root growth was assumed. The entire domain was initialized
251 in pressure head with an initial groundwater table at 250 cm and hydrostatic equilibrium with
252 the groundwater table in the unsaturated zone. In total, the simulation time was 22 years and
253 only the years 2000 to 2013 were taken for analysis to be independent from initialization. This
254 kind of spin-up is generally used in many modelling exercises to be independent of the initial
255 soil water conditions in the soil profile as shown by e.g., Boesten et al. (2007) or
256 Weihermüller et al. (2011).
257 First, the ET_a was calculated using HYDRUS 1D. Values were then compared to ET_G based
258 on the WTF method calculated from the groundwater fluctuations simulated by HYDRUS 1D.
259 For the modelling of the groundwater level fluctuations the van Genuchten parameters
260 obtained from inverse simulation of the HYPROP® data were used (Tab. 1) and the root water
261 uptake by the plants was calibrated in way that observed and modeled groundwater
262 fluctuations match each other as close as possible. In this respect, the root zone depth for the
263 perennial grassland and the parameter of critical water stress index for root water uptake were
264 adapted as proposed by Šimunek and Hopmans (2009). In a second step, modeled HYDRUS
265 1D derived ET_G were compared to calculations based on the WTF method from
266 measurements of the piezometer P3-1.

267 **2.5. Calculation of the groundwater decoupling depth**

268 The decoupling depth *d’* defines the depth of the water table, where the actual
269 evaportranspiration ET_a becomes lower as the potential evapotranspiration ET_0 because the
270 water demand of the atmosphere cannot be delivered totally from the groundwater reservoir
271 anymore. To estimate the decoupling depth *d’* and the decay coefficient *b* of the exponential

function the decline of the ratio ET_a/ET_0 with the water table depth was fitted by equation [12] to the ET_a and water table depth pairs according to Shah et al.(2007)

$$\frac{ET_a}{ET_0\ FAO\ PM} = \begin{cases} 1 & for\ WTD \leq d' \\ y_0 + e^{-b(WTD-d')} & for\ WTD > d' \end{cases} \quad [12]$$

where ET_a and ET_0 FAO-PM are the actual and reference evapotranspiration [cm], respectively, y_0 is the so called correction factor [-], and d' and b are constants [-], and WTD is the water table depth [cm].

2.6. Statistical analysis

Statistical analysis was performed to compare measured and modeled groundwater levels and the corresponding calculated ET_G rates. To indicate the goodness of the correlation the Pearsons correlation coefficient r and the root mean squared error (RMSE) were used. The coefficient of determination R^2 as the square of the Pearsons correlation coefficient was used to describe the goodness of fit for the regression analysis. In general, the RMSE can range from 0 to infinity, and lower values indicate better agreement between the two data sources (Willmott, 1981). Regression analysis were used to explain the relationship between ET_a and water table depth (WTD) for dry seasons of the years 2001 to 2013.

3. Results and Discussion

3.1. Soil texture and profile water content

The measured soil texture up to a depth of 300 cm is plotted in Fig. 2. As can be seen, the texture is dominated by 57% of fine sand (100-200 µm) and 14% of medium sand (200-250 µm) (Diouf, 2012). The measured gravimetric water contents are plotted in Fig 2a and were nearly constant between 0 and 200 cm depth with only ~ 4 to 6% and increase beyond to up to 18 % at 300 cm depth. The low gravimetric water contents between 0-200 cm could be expected, because sampling took place in the dry season of the year 2008. Additionally, water

295 content and percentage of fine particles exhibit a similar profile pattern (Fig. 2) except in the
296 top zone likely due to evapotranspiration losses of soil water.

297 **3.2. Soil hydraulic properties and specific yield**

298 Accurate knowledge of soil hydraulic properties is required in studying water flow in the
299 unsaturated zone. To obtain the hydraulic properties the HYPROP® data were inverted as
300 described in the Materials and Methods section. The best parameters of the inversion for the
301 different soil layers are listed in Tab. 1. As displayed, the saturated hydraulic conductivity of
302 the upper layer (0–25cm) is 570 cm d^{-1} and slightly decreases to 504 cm d^{-1} in the middle
303 layer (25–100cm), and 461 cm d^{-1} in the third layer (100–200cm), respectively. Saturated and
304 residual water content values ranged between 0.42 to 0.45 cm^3 cm^{-3} and 0.0011 to 0.0062 cm^3
305 cm^{-3}. The shape parameters α and n were also in the same order of magnitude in the three
306 layers. It has to be noted, that the soil layers were almost homogeneous, without obvious
307 small scale layering at least from visual inspection of the soil augers.

308 The estimating of water budget components, such as groundwater recharge and
309 evapotranspiration requires also accurate determination of the specific yield, which is a
310 crucial term in the WTF method (Chen et al., 2010; Fahle and Dietrich, 2014). The specific
311 yield values calculated using Eq. [3] and [4] varied between 0.29 and 0.33 depending on the
312 years analyzed. This is in good agreement with data presented by Loheide et al. (2005), who
313 reported specific yields of 0.32 when the depth to the water table exceeds 1 m.

314 **3.3. Temporal variability in groundwater level and ET**

315 ***Seasonal Groundwater level changes***

316 Figure 5 shows the HYDRUS 1D simulated groundwater levels for two different scenarios,
317 where the soil was either assumed to be bare or covered by short perennial grass. Both states
318 (bare and vegetated) are observed in the vicinity of the monitoring piezometer. Additionally,
319 water table fluctuations measured in the piezometer are plotted for the years 2010 to 2012. As
320 can be seen from the HYDRUS 1D modelled groundwater table fluctuations, each dry season

leads to a pronounced drop of the groundwater table and a relaxation in the corresponding wet season, whereby the drop nearly showed same levels for each year, independently of the maximum level of the groundwater table during the previous rainy season. Looking at the match between the modelled and measured groundwater tables for the years 2010 to 2012 indicates that the model results based on the assumption that the soil was bare is less good compared to the vegetated scenario. For better comparison, the modelled versus measured groundwater levels for the dry season are plotted in Fig. 6. For the bare soil assumption, the *r* is 0.96 with and RMSE of 0.26 m. On the other hand, for the grassland vegetation a slightly higher *r* (0.98) and a smaller RMSE of 0.12 m indicates that the grassland vegetation scenario is more adequate to describe the groundwater fluctuations in this area.

Simulated HYDRUS 1D ET_a and ET_G

The actual ET values obtained with the two methods, namely the direct ET_a output from HYDRUS 1D and the ET_G calculated by the WTF method based on simulated HYDRUS 1D water table fluctuations were compared in a first step to analyze the applicability and validity of the WTF method for this site. Table 2 presents result for each individually simulated dry season with regard to the cumulative rainfall from the previous rainy season, the total length of the dry season, and the maximum difference in groundwater level between wet and dry season. Data reveal that precipitation amounts vary greatly with a minimum of 272 mm in 2007 and a maximum of 723 mm in 2009 with a mean of 475 mm over all years. Length of the dry season also varies between 145 (2002) and 271 (2013) days (mean = 229 days). Drawdown varies as well and ranges from 18.1 (2002) to 113.2 (2013) cm (mean = 60 cm) for the bare soil scenario and from10.4 (2002) and 101.9 (2013) cm (mean = 54.4 cm) for the perennial grass scenario, whereby no significant correlation (p= 0.05) between length of the dry period and water table decline was observed. The generally lower values of the drawdown for the perennial grass scenario are probably caused by the generally lower water table during the wet season due to root water uptake during the vegetation period and a deeper

347 groundwater table during the dry season. HYDRUS 1D based ET_a varies for the bare soil
348 scenario between 0.22 (2003) and 1.11 (2013) mm d^{-1} with a mean of 0.60 mm d^{-1} and for the
349 perennial grass vegetation scenario between 0.23 (2002) and 1.28 (2011) mm d^{-1} with a mean
350 of 0.78 mm d^{-1}. Higher ET_a in this latter scenario can be explained by greater water extraction
351 due to root water uptake, especially from deeper soil layers. Because of variability in dry
352 season length, total cumulative ET_a (mm) varies accordingly. The total evaporation loss
353 during the dry season with respect to the rainfall recorded in the previous rainy season varies
354 from 10 % in 2002 to more than 47 % in 2013 (mean = 28 %), suggesting potential
355 groundwater recharge variability.
356 Looking at the results of ET_G calculated by the WTF method reflects the same pattern as for
357 the ET_a, whereby slightly higher ET_G (mean +0.23 mm d^{-1}) compared to ET_a was calculated
358 for the bare soil scenario. On the other hand, calculated ET_a and ET_G matched each other well
359 for the vegetated scenario with only a very small underestimation of ET_G (mean = -0.04 mm
360 d^{-1}). Mean ET_G over the entire dry periods was estimated to be 0.82 and 0.73 mm d^{-1} for the
361 bare and vegetated case, respectively, which is +37 and -6.5 % deviation from the direct
362 HYDRUS 1D calculated ET_a. The reason for the slightly larger differences between ET_G and
363 ET_a for the bare soil scenario are unclear, especially that measurement errors can be excluded
364 in the synthetic case shown. Therefore, one can question if the definition of the specific yield
365 as shown in Eq. 3 and 4 can be used globally. On the other hand, one can question why the
366 use of the same specific yield seems not to impact the vegetated scenario. Here, one can
367 speculate, that the additional water extraction form the root zone by the plants somehow
368 compensate the incorrectly defined specific yield. For a better insight into the direct
369 comparison between ET_a and ET_G both values were plotted versus each other in Fig. 7 for
370 both scenarios. Overall, a good agreement between both methods can be detected with high
371 R^2 values exceeding 0.98, whereby a general overestimation of the ET_G for the bare soil
372 conditions is again visible resulting in an RMSE of 0.23 mm d^{-1}. In comparison, and as

373 already stated, the ET_G and ET_a match well over the entire ET_a range for the vegetated
374 scenario (RMSE = 0.12 mm d^{-1}), which gives confidence that the WTF method can be used to
375 estimate actual evaporation during the dry season from piezometer data only in the study area,
376 when vegetation is present.
377 The calculated daily ET_a (0.23–1.28 mm d^{-1}) and ET_G (0.17–1.20 mm d^{-1}) values in our study
378 area were lower than other ET_G estimates for vegetated areas where the WTF method was
379 also applied. For example, Mould et al. (2010) estimated maximum ET_G rates of 5.91 mm d^{-1}
380 in Northern Germany, where the water table depth ranged only between 0.1 to 0.6 m,
381 indicating, that not only the atmospheric demand (Gribovszki et al., 2008) but also the total
382 water table depth, the soil properties of the vadose zone, as well as vegetation type determine
383 the absolute evapotranspiration (Cleverly et al., 2006; Cooper et al., 2006; Devitt et al., 2011).
384 However, our evapotranspiration values are comparable with estimated ET_G rates in semi-arid
385 and arid environments, where the groundwater table is in general much deeper. Pozdniakov et
386 al. (2013) and Lautz (2008) obtained ET_G values from 0.1 to 2 mm d^{-1} and 0.0 to 3.1 mm d^{-1}
387 (for short grass prairie) for water table depth ranged between 1.5 to 4 m and 1 to 3 m,
388 respectively. In a hyper-arid environment of northwestern China, Wang et al. (2014) and
389 Cheng et al (2017) obtained similar ET_G values (0.63 to 2.33 mm d^{-1}) from 0.5 to 3.5 m water
390 table depth. The results presented in this study are consistent with those presented by Gardner
391 (1958) who show that evaporation demand is mainly controlled by external condition and
392 water table depth.
393 ***ET_G from piezometer data and HYDRUS 1D simulation***
394 Daily ET_G values estimated from measured groundwater levels in the piezometer and the
395 WTF method varies between 0.84 (2012) and 1.34 mm d^{-1} (2011) with a mean of 1.10 mm d^{-1}.
396 ET_G of the year 2011 is higher than the ET_a modeled in bare soil condition (29 % mismatch)
397 but is in the same range as the ET_a modeled in the vegetated scenario assuming a perennial
398 grass cover (5 % mismatch). However, in 2012 the difference between ET_a and ET_G is much

399 larger with nearly three-fold ET_G compared to the bare soil ET_a and an overestimation of 42
400 % for the vegetated ET_a. The mismatch for the year 2012 can be attributed to the fact that the
401 measured groundwater fluctuations were not recorded for the entire dry season and ended
402 already at April, 7th 2012. Even if only one dry season was completely covered by the
403 measurements, confidence in the WTF method for this study area is given by the synthetic
404 model study using the HYDRUS 1D simulations.

405 ***Relationship between ET_a, ET_0, and WTD***

406 The daily potential evapotranspiration ET_0 is only poorly related to daily ET_a ($R^2 < 0.08$)for
407 the two scenarios (bare and vegetated), but in general, higher daily ET_a rates correspond to
408 higher daily ET_0 and modeled ET_a equals the ET_0 FAO-PM when the groundwater table is
409 shallow corresponding to the end of the rainy season (October - November). The same has
410 been already shown by Kurc and Small (2004), who found that in semi-arid ecosystems, the
411 maximum ET_a rate during the dry season occurs immediately after the rainy season and then
412 rapidly decreases within days of no additional rainfall.

413 In a next step, simulated ET_a data were plotted against the water table depth (WTD) for each
414 single year for further analysis. Figure 8 clearly shows that ET_a values are highly related to
415 water table depth and could be described by an exponential function with an $R^2 = 0.80$ over
416 all years. Largest regression between ET_a and WTD occurred in the years 2001 ($R^2 = 0.84$),
417 2006 ($R^2 = 0.83$), 2009 ($R^2 = 0.85$), 2010 ($R^2 = 0.73$), 2011 ($R^2 = 0.88$), and 2013 ($R^2 = 0.84$),
418 where the WTD was most shallow due to the large precipitation amounts in the previous rainy
419 season but also spans a more or less wide range. On the other hand, the relationships was poor
420 for the year 2002 ($R^2 = 0.23$) and 2003 ($R^2 = 0.35$), where the WTD was low and nearly no
421 fluctuations were detectable. In conclusion, ET_a seems to be mainly driven by the water table
422 depth at this site. The influence of WTD in evapotranspiration demand is also noted by
423 O'Connor et al. (2019) and Gao et al. (2017) in a study conducted over different land covers.

Figure 9 shows the plot of ET_a rates vs. WTD for the simulation with perennial grass cover and for all years. The simulated ET_a was normalized by the ET_0 FAO-PM. Therefore, the ratio ET_a/ET_0FAO-PM varied only between 0 and 1. As can be seen, the ET_a is equal to potential evapotranspiration until the water table reaches a depth *d'*, defined as the decoupling depth by Shah et al. (2007). Up to this critical depth, the aquifer will provide most part of water for ET_a. In our case, the decoupling depth equal 1.46 m. Beyond this point, ET_a shifts from atmospheric control (ET_a is equal to ET_0) to soil-moisture control of the vadose zone. Again, below the transition depth, ET_a decreased with decreasing WTD in an exponential way. The same observations was shown in the previous works of Shah et al. (2007), who proposed an exponential relationship for evaporation from a shallow water table from different land covers and soils.

First, equation [14] was used, without tacking into account the correction factor y_0, to simulate the decline of ET_a with decline in WTD. In the fitting process, the decoupling depth was assuming to equal 1.46 m as shown in Figure 9. The exponential function fitted well the data for shallow water table, but the fit was poor with an $R^2$of 0.59 and a RMSE of 0.121 m for WTD >*d'*. Introducing a correction factor enhanced the fitted model (R^2 = 0.78; RMSE = 0.035 m). The correction factor (y_0) and the decay coefficient (b) values obtained in this study are different than those obtained by Shah et al. (2007) in grass cover and for sandy soils probably due to differences in decoupling depth and soil characteristics.

4. Conclusion

Daily groundwater level fluctuations were observed during the dry season in Dakar area. The modelled data showed groundwater table drawdown from 18.1 to 113.2 cm and 10.4 to 101.9 cm for bare soil and perennial grass scenario, respectively. The results also indicate that each dry season leads to a pronounced drop of the groundwater table and this drop nearly showed same levels for each year, independently of the maximum level of the groundwater table

449 during the previous rainy season. Additionally, dry season ET_a as an important component of
450 the annual water balance consumed 10 to 43 % of annual rainfall for this site.
451 Modeled daily groundwater levels were first used to quantify ET_G and to analyze the
452 applicability and validity of the WTF method for this site. Modelled actual evapotranspiration
453 (ET_a) ranged between 0.22 to 1.28 mm d^{-1}. The comparison of ET_a and ET_G values obtained
454 for the vegetated scenario show that the WTF method can be used to estimate actual
455 evaporation during the dry season from piezometer data only in the study area.
456 Furthermore, daily ET_a is directly coupled to the water table depth (WTD), whereby
457 shallower WTD increased ET_a irrespectively of the atmospheric demand. Over all years, the
458 dependence between ET_a and WTD could be well described (R^2 = 0.80) by an exponential
459 function.
460 The simulated ET_a model shows that higher ET_a values occurred during the period from
461 October to December and lowers values were observed at June corresponding respectively to
462 the ends of the rainy and the dry season. Groundwater evapotranspiration estimation based on
463 the modeling and WTF methods may be considered the simplest, easiest, and least expensive
464 technique available but the method involves a number of sources of uncertainty (Soylu et al.,
465 2012). In addition, a reliable quantification of actual evapotranspiration requires a
466 comprehensive investigation that combines the modeling approach with traditional methods,
467 such as weighable lysimeters and eddy correlation method.

468 **5. Acknowledgement**

469 This study was financially supported by a Post-Doctoral Grant from the German Academic
470 Exchange Service (DAAD) to Ousmane Coly Diouf at Forschungszentrum Jülich GmbH,
471 Agrosphere Institute IBG-3. The authors are grateful to the DAAD for this funding
472

6. References

Allen, R.G., Pereira, L.S., Raes, D., and Smith, M., 1998. Crop evapotranspiration, guidelines for computing crop water requirements, Vol. 56 of FAO Irrigation and Drainage. FAO, Rome, Italy, URL http://www.fao.org/docrep/X0490E/x0490e06.htm.

Bellion, Y.J.C., 1987. Historique géodynamique post-paléozoïque de l'Afrique de l'ouest d'après l'étude de quelques bassins sédimentaires (Sénégal, Taoudenni, Iullemmeden, Tchad). Thèse de Doctorat ès Sciences, Université d'Avignon (Paris, France), 302 p.

Bethenod, O., Katerji, N., Goujet, R., Bertolini, J. M., & Rana, G., 2000. Determination and validation of corn crop transpiration by sap flow measurement under field conditions. Theoretical and Applied Climatology, 67, 153−160.

Bobée, C., Ottlé, C., Maignan, F., de Noblet-Ducoudré, N., Maugis, P., Lézine, A. M,. Ndiaye, M., 2012. Analysis of vegetation seasonality in Sahelian environments using MODIS LAI, in association with land cover and rainfall. Journal of Arid Environments *(84)* 38-50

Boesten, J.J.T.I. 2007. Simulation of pesticide leaching in the field and in zero tension lysimeters. Vadose Zone J. 6: 793–804. doi:10.2136/vzj2007.0067.

Carlson Mazur, M. L., Wiley, M. J., and Wilcox D. A., 2014. Estimating evapotranspiration and groundwater flow water-table fluctuations for a general wetland scenario. Ecohydrology. 7, 378–390.

Castalain, J., 1965**.** Aperçu stratigraphique et micropaléontologique du bassin du Sénégal. Historique de la découverte paléontologique. *In* Coll. Int. de micropaléontologie, Dakar et mémoire BRGM n032, p.357-365, 1pl. h.t.

Chen, X., Song, J., Wang, W., 2010. Spatial variability of specific yield and verticalhydraulic conductivity in a highly permeable alluvial aquifer. Journal of Hydrology388 (3–4), 379–388.

498 Cheng, D., Duan, J., Qian, K., Qi, L., Yang, H,, Chen, X. 2017. Groundwater
499 evapotranspiration under psammophilous vegetation covers in the Mu Us Sandy Land,
500 northern China. Journal of Arid Land, 9(1): 98–108. doi: 10.1007/s40333-016-0095-7.

501 Cleverly, J.R., Dahm, C.N., Thibault, J.R., McDonnell, D.E., Allred Coonrod, J.E., 2006.
502 Riparian ecohydrology: regulation of water flux from the ground to theatmosphere in
503 the Middle Rio Grande, New Mexico. Hydrological. Processes 20 (15),3207–3225.

504 Cooper, D.J., Sanderson, J.S., Stannard, D.I., Groeneveld, D.P., 2006. Effects of longterm
505 water table drawdown on evapotranspiration and vegetation in an arid region
506 phreatophyte community. Journal of Hydrology 325 (1–4), 21–34.

507 Crosbie, R.S., Binning, P., Kalma, J.D., 2005. A time series approach to inferringgroundwater
508 recharge using the water table fluctuation method. Water Resources Research 41 (1),
509 W01008.

510 Devitt, D.A., Fenstermaker, L.F., Young, M.H., Conrad, B., Baghzouz, M., Bird, B.M., 2011.
511 Evapotranspiration of mixed shrub communities in phreatophytic zones of the Great
512 Basin region of Nevada (USA). Ecohydrology 4 (6), 807–822.

513 Diouf, O.C., Faye, S.C., Dieng, N.M., Faye, S., Faye, A., Englert, A., Wohnlich, S., 2013.
514 Hydrological Risk Analysis with Optical Remote Sensing and Hydrogeological
515 Modelling: Case Study of Dakar Flooding Area (Senegal). Geoinformatic and
516 Geostatistic: An Overview, S1http://dx.doi.org/10.4172/2327-4581.S1-011.

517 Diouf, O.C., 2012. Apport des outils cartographiques et géochimiques à la validation des
518 paramétres d'entrées du modéle hydrogéologique de la nappe des sables quaternaires de
519 Dakar: implication sur les inondation en zone péri-urbaine. Thèse de doctorat unique,
520 Université Cheikh Anta Diop de Dakar, 221p.

521 Duke, H., 1972. Capillary properties of soils – influence upon specific yield. Transactions of
522 the American Society of Agricultural Engineers. 15, 688–691.

523 Engel, V., Jobbágy, E.G., Stieglitz, M., Williams, M., Jackson, R.B., 2005.
524 Hydrologicalconsequences of Eucalyptus afforestation in the Argentine Pampas. Water
525 Resources Research 41 (10), W10409.

526 Fahle, M., Dietrich, O., 2014. Estimation of evapotranspiration using diurnal groundwater
527 level fluctuations: comparison of different approaches with groundwater lysimeter data.
528 Water Resources Research50 (1), 273–286

529 February, E.C., Higgins, S.I., 2010. The distribution of tree and grass roots in savannas in
530 relation to soil nitrogen and water. South African Journal of Botany. 76: 517–
531 523Feddes, R. A., Bresler, E., Neuman, S. P., 1978. Field test of a modified numerical
532 model for water uptake by root systems. Water Resources Research, 10, 1199-1206.

533 Gao, X., Huo, Z., Qu, Z., Xu, X., Huang, G., & Steenhuis, T. S. 2017. Modeling contribution
534 of shallow groundwater to evapotranspiration and yield of maize in an arid area. 2017
535 Scientific Reports | 7:43122 | DOI: 10.1038/srep 43122.

536 Gerla, P.J., 1992. The relationship of water-table changes to the capillary fringe,
537 evapotranspiration, and precipitation in intermittent wetlands. Wetlands 12:91–98.

538 Gribovszki, Z., Kalicz, P., Szilágyi, J., Kucsara, M., 2008.Riparian zone evapotranspiration
539 estimation from diurnal groundwater level fluctuations.Journal of Hydrology. 349 (1–2),
540 6–17.

541 Gribovszki, Z., Szilágyi, J., Kalicz, P., 2010. Diurnal fluctuations in shallow groundwater
542 levels and streamflow rates and their interpretation – a review.Journal of Hydrology.
543 385 (1–4), 371–383

544 Hargreaves, G.H., and Samani, Z.A., 1985. Reference crop evapotranspiration from
545 temperature. Applied engineering in agriculture1 (2), 96-99.

546 Healy, R.W., Cook, P.G., 2002. Using groundwater levels to estimate recharge. Hydrogeology
547 Journal, 10: 91-109.

548 Hsiao, T., &Xu, L., 2005.Evapotranspiration and relative contribution by thesoil and the
549 plant. California water plan update 2005 : UC Davis.

550 Kollett, S, J., Cvijanovic, I., Schüttemeyer, D., Maxwell, R.M., Moene, A.F., and Bayer, P.,
551 2009. The influence of rain sensible heat and subsurface energy transport on the energy
552 balance at the land surface. Vadose Zone Journal. 8: 846-857.

553 Kurc, S. A., Small, E. E., 2004. Dynamics of evapotranspiration in semiarid grassland and
554 shrubland ecosystems during the summer monsoon season, central New Mexico. Water
555 Resources Research 40(9), W0930515. DOI10.1029/2004WR003068

556 Lautz, L. K., 2008. Estimating groundwater evapotranpiration rates using diurnal water-table
557 fluctuations in a semi-arid riparian zone. Hydrogeology Journal. 16, 483 – 497,
558 doi:10.1007/s10040-007-0239-0.

559 Loheide, S.P., Butler Jr, J.J., and Gorelick, S.M., 2005. Estimation of groundwater
560 consumption by phreatophytes using diurnal water table fluctuations: A saturated-
561 unsaturated flow assessment. Water Resources Research. 41: doi:
562 10.1029/2005WR003942.

563 Loheide II, S.P., 2008. A method for estimating subdaily evapotranspiration of shallow
564 groundwater using diurnal water table fluctuations. Ecohydrology 1 (1), 59–66.

565 Maignien, R., 1959. Les sols de la presqu'île du Cap-Vert. Rapport technique Office de la
566 Recherche Scientifique et Technique d'Outre-mer (ORSTOM) Dakar-Hann. 163p.

567 Makkink, G.F., 1957. Testing the Penman formula by means of lysimeters. Journal of
568 Institution of Water Engineers 11, 277–288.

569 Mazur, M. L. C., Wiley, M. J., and Wilcox, D. A., 2014. Estimating evapotranspiration and
570 groundwater flow from water-table fluctuations for a general wetland scenario.
571 Ecohydrology.7, 378–390. DOI: 10.1002/eco.1356.

572 Maxwell, R.M. and Kollet, S.J., 2008 Interdependence of groundwater dynamics and land-
573 energy feedbacks under climate change. Nature Geoscience 1(10): 665-669.

574 Meissner, R., Seeger, J., Rupp, H., Seyfarth, M., and Borg, H., 2007.Measurement of dew,
575 fog, and rime with a high precision gravitation lysimeter. Journal of Plant Nutrition and
576 Soil Science. 170: 335-344.

577 Meyboom, P., 1965. Three observations on streamflow depletion by phreatophytes. Journal of
578 Hydrology 2 (3), 248–261.

579 Moffat, A.M., Papale, D., Reichstein, M., Hollinger, D.Y., Richardson, A.D., Barr, A.G.,
580 Beckstein, C., Braswell, B.H., Churkina, G., Desai, A.R., Falge, E., Gove, J.H.,
581 Heimann, M., Jarvis, A.J., Kattge, J., Noormets, A., and Stauch, V.J., 2007.
582 Comprehensive comparison of gap-filling techniques for eddy covariance net carbon
583 fluxes. Agricultural and Forest Meteorology. 147: 209-232.

584 Mould, D. J., Frahm, E., Salzmann, T., Miegel, K., and Acreman, M. C., 2010. Evaluating the
585 use of diurnal groundwater fluctuations for estimating evapotranspiration in wetland
586 environments: Case studies in Southeast England and Northeast Germany,
587 Ecohydrology, 3(3), 294–305.

588 Nichols, W.D., 1994. Groundwater discharge by phreatophyte shrubs in the Great Basin as
589 related to depth to groundwater. Water Resources Research30:3265–3274.

590 O'Connor, J., Santos, J.M., Rebel, K.T. and Stefan C. Dekker, S.C. 2019. The influence of
591 water table depth on evapotranspiration in the Amazon arc of deforestation. Hydrology
592 and Earth System Sciences., 23, 3917–3931, https://doi.org/10.5194/hess-23-3917-
593 2019.

594 Pozdniakov, S., Wang P., Grinevskiy, S., Yu.; J., 2013. Simulation of Groundwater
595 Evapotranspiration with HYDRUS-1D in Desert Environments. Proceedings of the 4th
596 International Conference HYDRUS Software Applications to Subsurface Flow and
597 Contaminant Transport Problems, pp 289-297.

598 Priestley, C.H.B., and Taylor, R.J., 1972. On the assessment of surface heat flux and
599 evaporation using large scale parameters. Monthly Weather Review 100, 81-92.

600 Ridolfi, L., D'Odorico, P., and Laio, F., 2007. Vegetation dynamics induced by phreatophyte-
601 aquifer interactions. Journal of Theoretical Biology. 248(2): 301-310.

602 Ridolfi, L., D'Odortico, P., and Laio, F. 2006. Effect of vegetation – water table feedbacks on
603 the stability and resilience of plant ecosystems. Water Resources Research 42, W01201,
604 Doi: 10. 1029/2005WR004444.

605 Sanderson, J.S. and Cooper, D.J., 2008. Groundwater discharge by evapotranspiration in
606 wetlands of an arid intermountain basin. Journal of Hydrology 351: 344 - 359. DOI:
607 10.1016/j.jhydrol. 2007. 12.023.

608 Schindler, U., Durner, W., von Unold, G. and Müller, L., 2010. Evaporation method for
609 measuring unsaturated hydraulic properties of soils: Extending the measurement range.
610 Soil Science Society of America Journal.74 (4): 1071-1083.

611 Schrader, F., Durner, W., Fank, J., Gebler, S., Pütz, T., Hannes, M., and Wollschläger, U.,
612 2013. Estimating precipitation and actual evapotranspiration from precision lysimeter
613 measurements. In: Romano, N., D'Urso, G., Severino, G., Chirico, G., and Palladino,

M. (Eds.). Four Decades of Progress in Monitoring and Modeling of Processes in the Soil-Plant-Atmosphere System: Applications and Challenges. Procedia Environmental Sciences: 543–552.

Shah, N., Nachabe, M., and Ross, M., 2007.Extinction depth and evapotranspiration from groundwater under selected land covers. Ground Water 45 (3), 329–338

Šimůnek, J., van Genuchten, M. T., and Šejna, M., 2008. Development and applications of the HYDRUS and STANMOD software packages and related codes. Vadose Zone Journal, **7**(2), 587-600.

Šimůnek, J., andvan Genuchten,M. T.,2008. Modelling non-equilibrium flow and transport processes using HYDRUS. Vadose Zone Journal, **7**, 782-797.

Šimůnek, J., and Hopmans, J.W., 2009. Modeling compensated root water and nutrient uptake. Ecological Modelling 220 (4), 505–521.

Sophocleous, M., 1985.The role of specific yield in groundwater recharge estimations: A numerical study. Vol. 23; n° 1- Groundwater, pp 53-58.

Soylu, M.E., Lenters, J.D., Istanbulluoglu, E., and Loheide II, S.P., 2012. On evapotranspiration and shallow groundwater fluctuations: a Fourier-based improvement to the White method. Water Resources Research. 48 (6), W06506.

Thornthwaite, C.W., 1948. An approach toward a rational classification of climate. The Geographical Review, 38 (1), 55-94.

Troxell, H., 1936. The diurnal fluctuation in the ground-water and flow of the Santa Ana River and its meaning. Transactions, American Geophysical Union 17 (4), 496–504.

Twine, T.E., Kustas, W.P., Norman, J.M., Cook, D.R., Houser, P.R., Meyers, T.P. Prueger, J.H., Starks, P.J., and Wesely, M.L., 2000. Correcting eddy-covariance flux underestimates over a grassland. Agricultural and Forest Meteorology.103: 279-300.

638 Vanderborght, J., Graf, A., Steenpass, C., Scharnagl, B., Prolingheuer, N., Herbst, M.,
639 Hendricks-Franssen, H.-J., and Vereecken, H., 2010. Within-field variability of bare soil
640 evaporation derived from eddy covariance measurements. Vadose Zone Journal. 9: 943-
641 954.

642 Van Genuchten, M. T., 1980. A closed-form equation for predicting the hydraulic
643 conductivity of unsaturated soils. Soil Science Society of America Journal, 44, 892–
644 898.

645 Von Unold, G., and Frank, J., 2008. Modular design of field lysimeters for specific
646 application needs. Water Air and Soil Pollution Focus. 8: 233-242.

647 Wang, P., Grinevsky, S.O., Pozdniakov, S.P., Yu, J., Dautova, D.S., Min, L., Chaoyang, D.,
648 Zhang, Y., 2014. Application of the water table fluctuation method for estimating
649 evapotranspiration at two phreatophyte-dominated sites under hyper-arid environments.
650 Journal of Hydrology 519 (2014) 2289–2300

651 Wang, P., Yu, J., Pozdniakov, S.P., Grinevsky, S.O., and Liu, C., 2014. Shallow groundwater
652 dynamics and its driving forces in extremely arid areas: a case study of the lower Heihe
653 River in northwestern China. Hydrological Processes 28 (3), 1539–1553.

654 Weihermüller, L., R. Kasteel, J. Vanderborght, J. Šimůnek, and H. Vereecken. 2011.
655 Uncertainties in pesticide monitoring using suction cups: Evidences from numerical
656 simulations. Vadose Zone Journal. 10: 1287-1298.

657 White, W.N., 1932. A Method of Estimating Ground-water Supplies Based on Discharge by
658 Plants and Evaporation from Soil: Results of Investigation in Escalante Valley, Utah,
659 Washington DC, US Geological Survey. Water Supply Paper 659-A, United States
660 Department of the Interior

661 Willmot, C.J., 1981. On the validation of models. Physical Geography, 2, 184-194.

662 Wilson, K. B., Hansonb, P. J., and Baldocchi, D. D., 2000.Factors controlling evaporation and
663 energy partitioning beneath a deciduous forest over an annual cycle. Agricultural and
664 Forest Meteorology, 102, 83−103.

665 Wilson, K., Goldstein, A., Falge, E.,Aubinet, M., Baldocchi, D., Berbigier, P., Bernhofer, C.,
666 Ceulemans, R., Dolman, H., Field, C., Grelle, A., Ibrom, A., Law, B.E., Kowalski, A.,
667 Meyers, T.,Moncrief, J., Monson, R., Oechel, W., Tenhunen, J., Valentini, R., and
668 Verma S., 2002. Energy balance closure at FLUXNET sites. Agricultural and Forest
669 Meteorology. 113: 223-243.

List of Tables

Tables

Table 1. Van Genuchten parameters obtained from HYPROP® data for the different soil layers. *Ks* was estimated independently using the falling head method. Note that the tortuosity *l* [-] was not fitted and set to 0.5.

Layers	θ_r [$cm^3\ cm^{-3}$]	θ_s [$cm^3\ cm^{-3}$]	α [cm^{-1}]	n [-]	Ks [$cm\ d^{-1}$]	l [-]
1 (0-25 cm)	0.0062	0.44	0.023	2.6	570	0.5
2 (25-100 cm)	0.0011	0.42	0.026	2.8	504	0.5
3 (100-200 cm)	0.0011	0.45	0.027	1.8	461	0.5

Table 2: Rainfall [mm], length of dry season [days], maximum difference in groundwater fluctuation ΔH [cm], and evapotranspiration rates (ET_a and ET_G) [mm d^{-1}] and cumulative evaporation (ET_a and ET_G) [mm] for different years.

				Without plant (bare soil)					With perennial Grass					Measurements	
years	Period	Rainfall [mm]	days	ΔH [cm]	ET_a HYDRUS		ET_G WTF		ΔH [cm]	ET_a HYDRUS		ET_G WTF		ΔH [cm]	ET_G WTF
					mm d^{-1}	mm	mm d^{-1}	mm		mm d^{-1}	mm	mm d^{-1}	mm		
2000		482													
2001	20 Oct-23 June	411	246	66.3	0.61	149.7	0.86	212.2	59.1	0.78	194.1	0.76	189.2		
2002	11 Jan-5 June	332	145	18.1	0.28	40.9	0.39	57.8	10.4	0.23	33.1	0.23	33.3		
2003	15 Dec-27 June	450	194	29.6	0.22	42.2	0.49	94.8	16.8	0.34	65.6	0.27	53.7		
2004	23 Oct-3 June	291	224	54.5	0.54	121.0	0.78	174.4	39.5	0.64	144.8	0.56	126.4		
2005	8 Oct-27 June	589	262	44.3	0.27	71.7	0.54	141.7	43.8	0.54	142.13	0.53	140.3		
2006	25 Oct-2 June	374	220	88.2	1.08	239.7	1.28	282	78.6	1.16	257.4	1.14	251.6		
2007	16 Oct-13 June	272	240	43.6	0.36	86.9	0.58	139.3	44.8	0.68	164.1	0.60	143.2		
2008	29 Sept-15 June	608	260	38.1	0.26	69.6	0.47	121.9	38.2	0.51	133.3	0.47	122		
2009	28 Oct-13 June	723	233	86.2	0.90	212.9	1.18	275.8	72.6	1.00	235.3	1.00	232.4		
2010	4 Dec-24 June	595	202	69.4	0.87	177.2	1.10	222.1	66.8	1.11	224.8	1.06	213.8		
2011	22 Oct-24 June	305	245	92.1	1.04	256.5	1.20	294.6	91.6	1.28	307.4	1.20	293.1	102.7	1.34
2012	19 Oct-15June	640	240	36.8	0.27	65.4	0.50	117.7	43.3	0.59	143.5	0.58	138.5	45.10	0.84
2013	2 Oct-30June	581	271	113.2	1.11	303.4	1.34	362.3	101.9	1.27	345.4	1.20	325.9		
Mean		475	229	60.0	0.60	141.3	0.82	192	54.4	0.78	183.9	0.73	174.1	73.9	1.10

Table 3: Fitted parameters of the exponential model (Eq. 14).

	d' (m)	b (m^{-1})	y_0 (-)	R^2	RMSE
without correction factor y_0	1.46	5.53		0.59	0.121
Fitting all parameters (d' and b)	0.88	1.78		0.74	0.035
Including correction factor y_0	1.46	0.37	-0.67	0.78	0.035

List of Figures

Figures

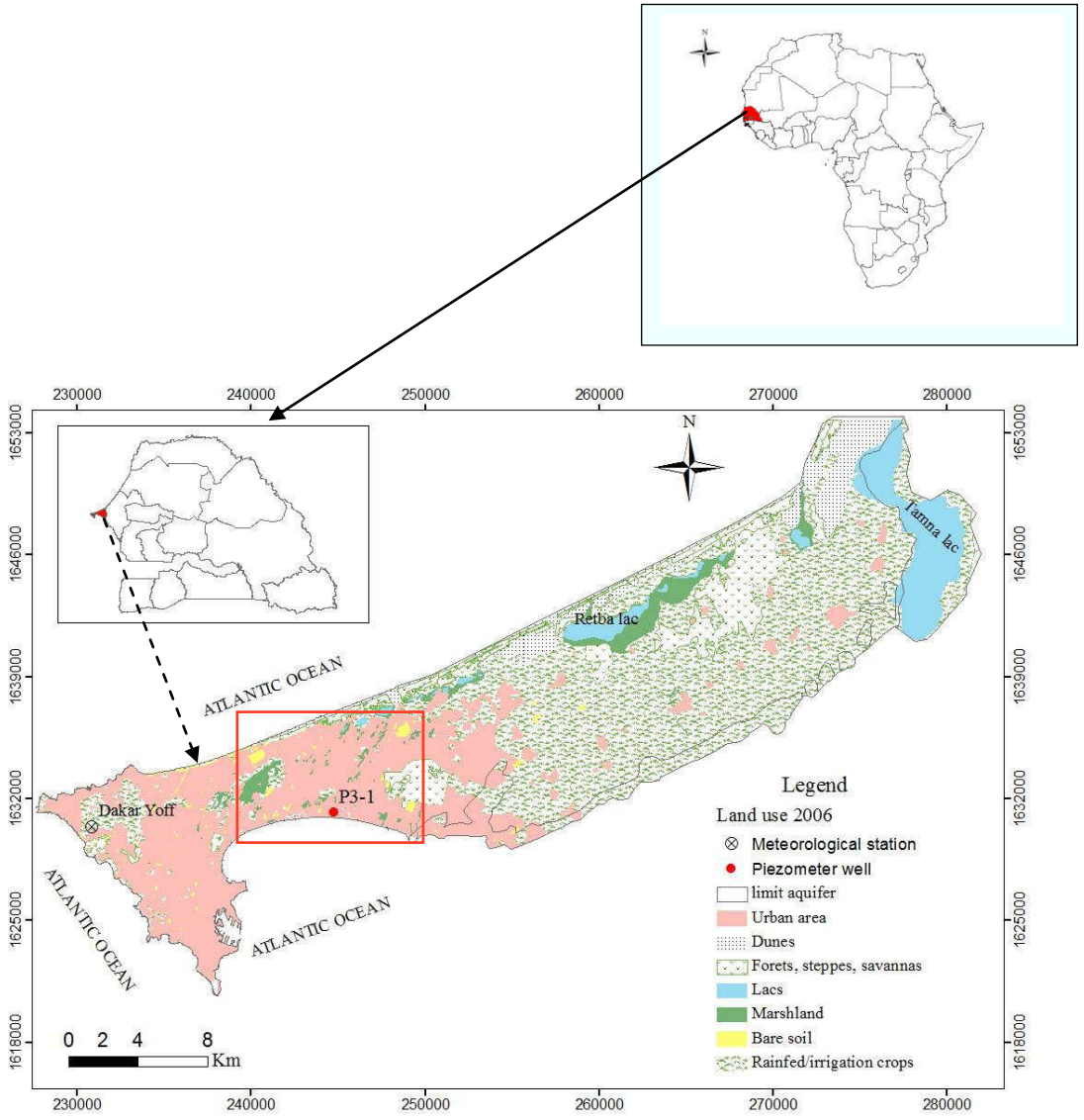

Figure 1.Land use and monitoring well location in the study area (red box).

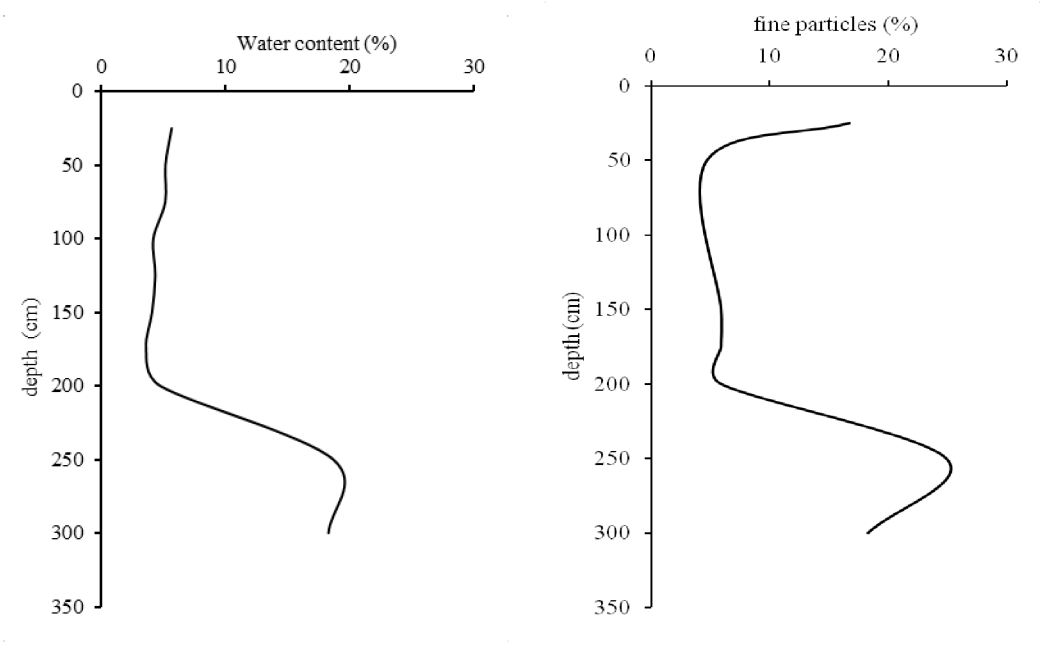

Figure 2. Gravimetric water content (%) (left) and fine particles (>50µm) distribution (%) (right) over depth of the soil profile.

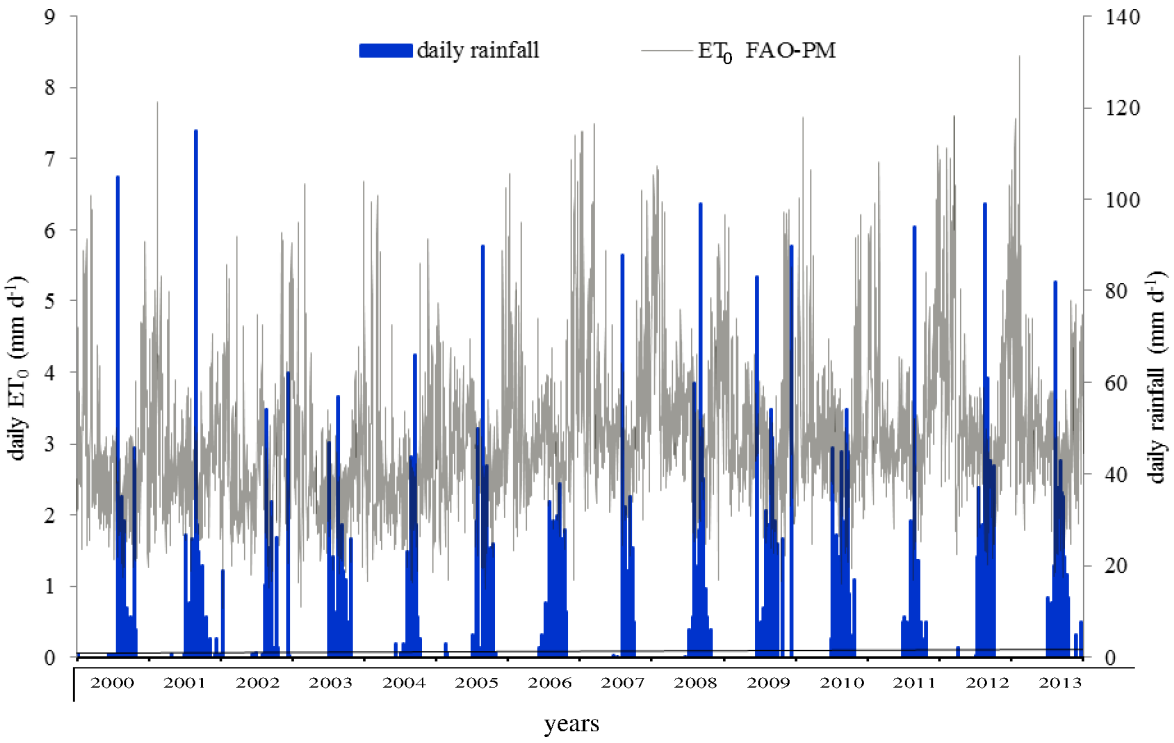

Figure 3.Daily ET_0 estimates of FAO-PM and daily rainfall for the time period 2000 to 2013.

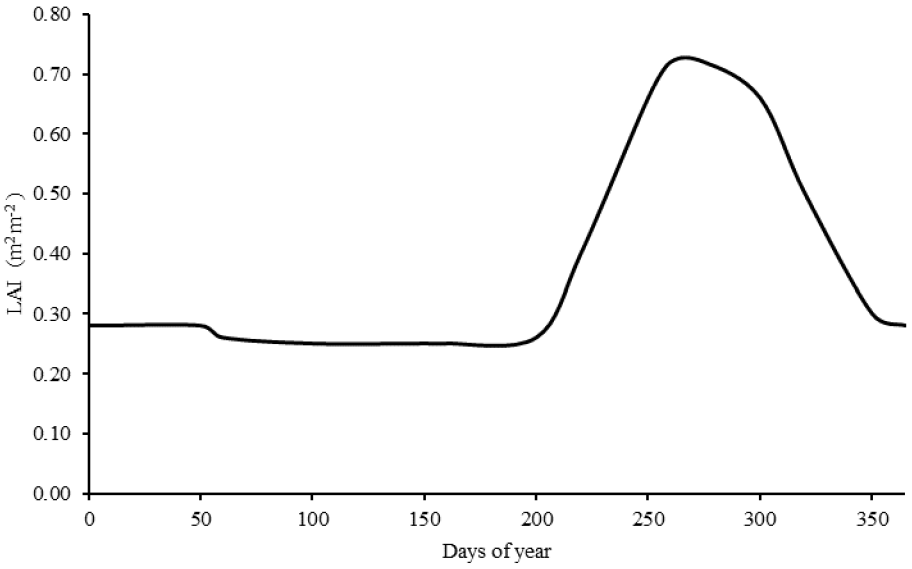

Figure 4. LAI averages for the period 2001 to 2008 in natural herbaceous savanna type vegetation (closed to open >40%) according to Bobée et al. (2012).

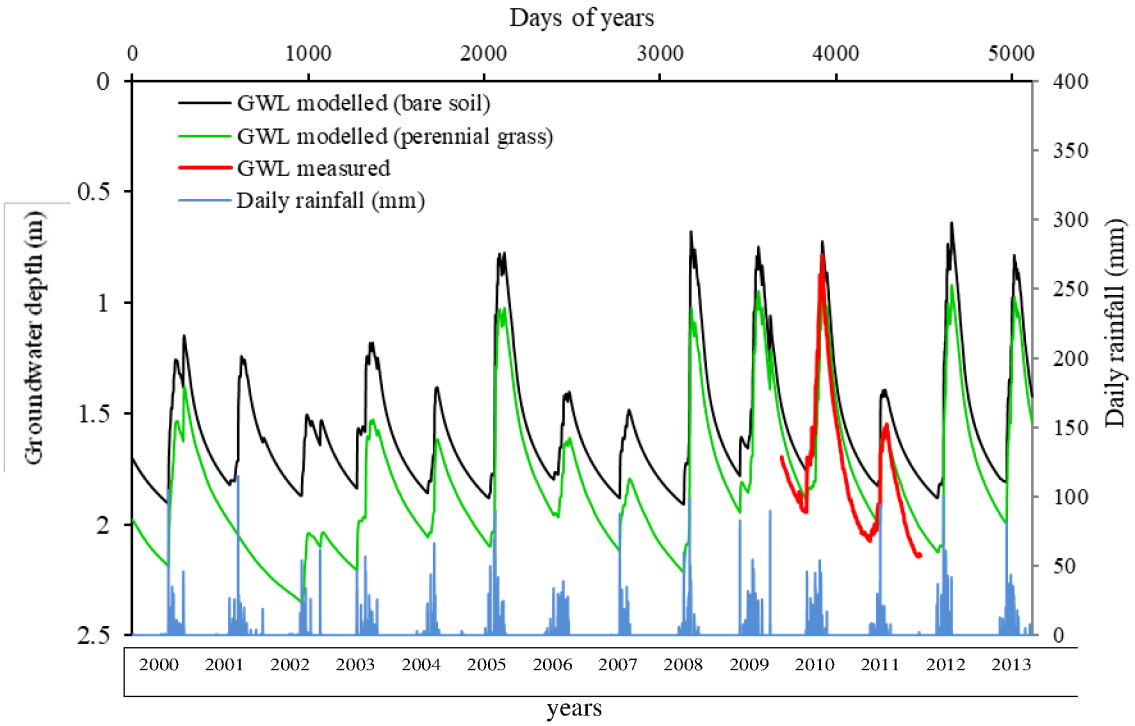

Figure 5. Daily rainfall and daily groundwater levels monitored (2010-2012) and modeled (2000-2013) for an urbanized (bare soil) and vegetated scenario for piezometer P3-1.

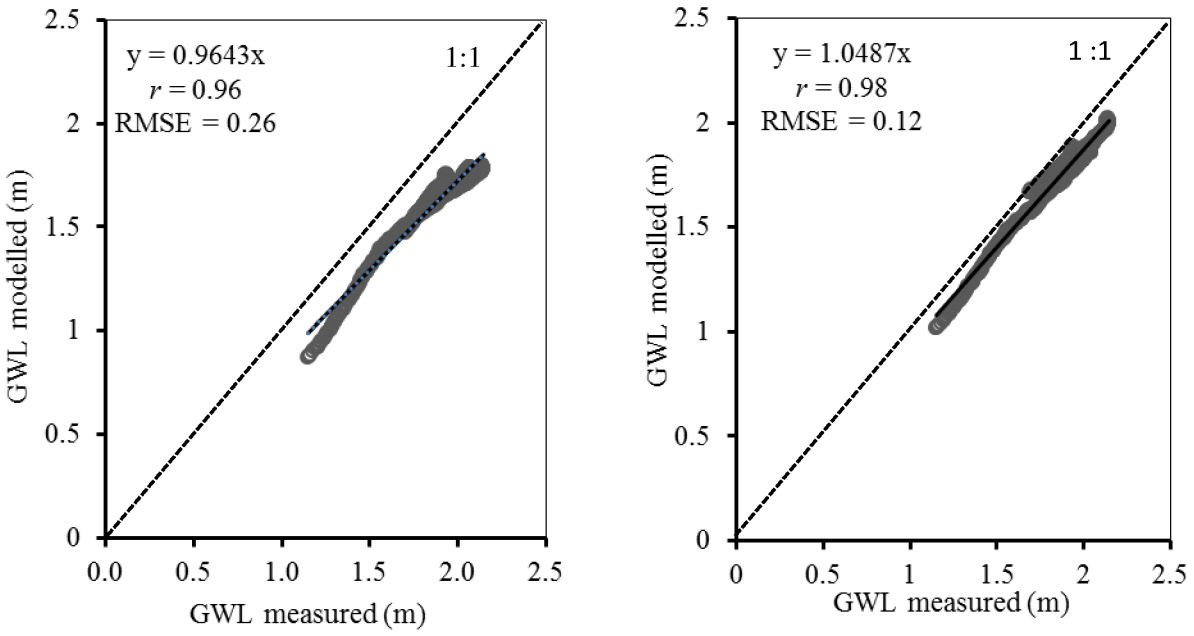

Figure 6. Correlation between daily groundwater levels (GWL) modelled vs measured (2010-2012) for the bare soil (left) and vegetative (right) conditions for piezometer P3-1 for the dry season.

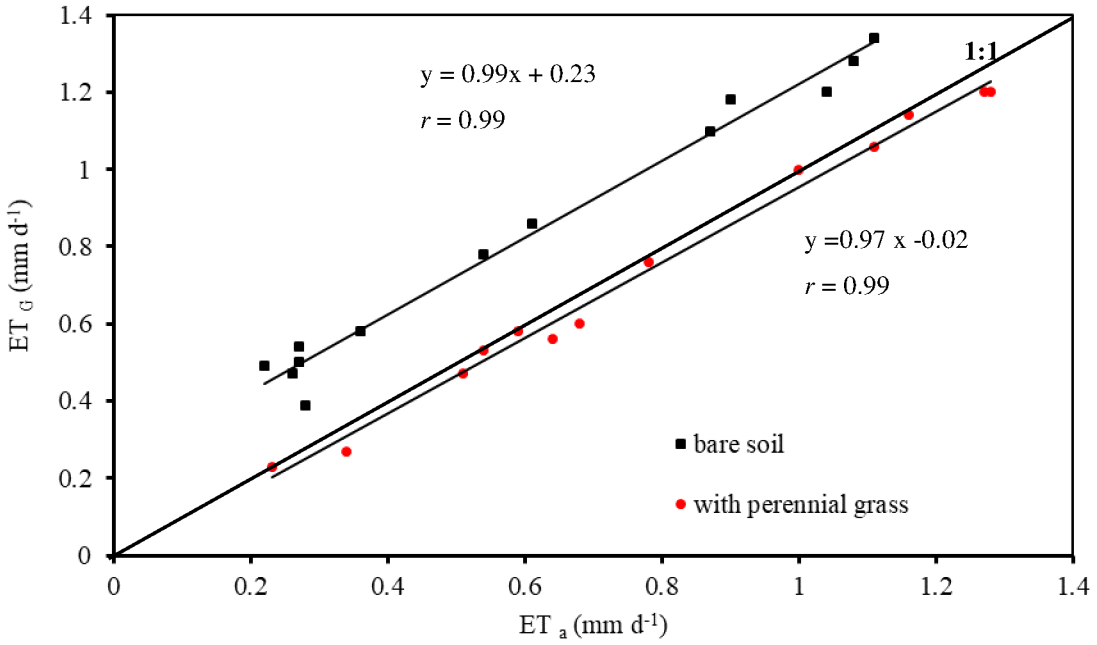

Figure 7: HYDRUS 1D derived ET_a versus WTF method computed ET_G [mm d^{-1}] for the bare soil and vegetated (perennial grass) scenario for the years 2001 to 2013.

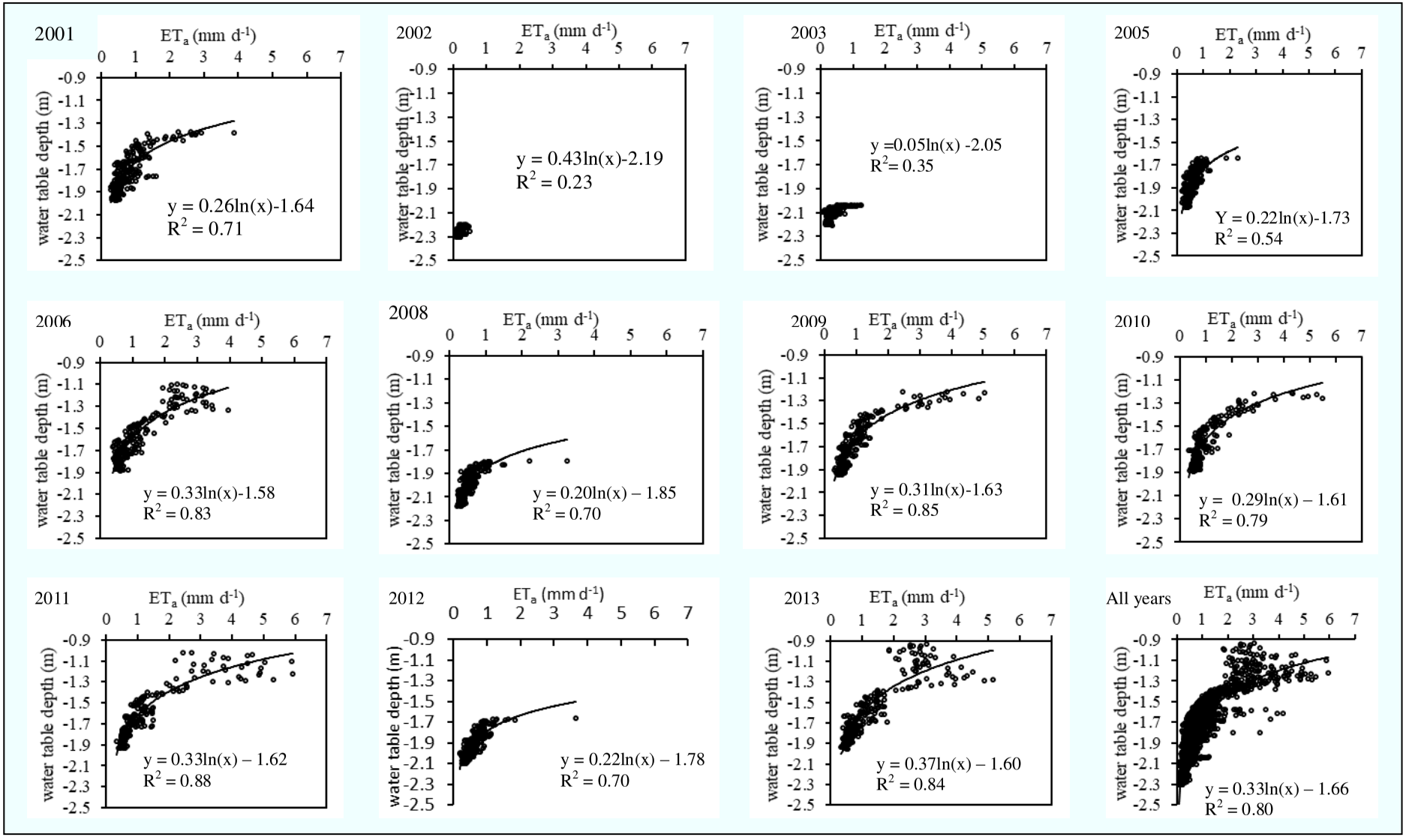

Figure 8: Relationship between ET_a and water table depth (WTD) for dry seasons of the years 2001 to 2013 and all years combined. Lines shown are exponential function regression

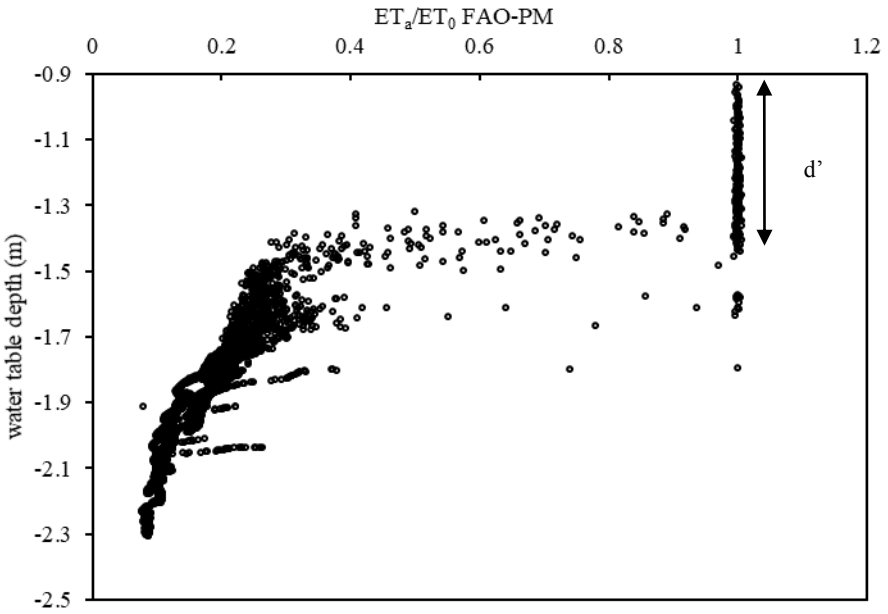

Figure 9.Variation of ratio of ET_a/ET_0 FAO-PM with water table depth for the vegetated scenario. Line shows the decoupling depth *d'* of 1.46 m.